Title

Phosphatidic acid affects structural organization of phosphatidylcholine liposomes. A study of 1,6-diphenyl-1,3,5-hexatriene (DPH) and 1-(4-trimethylammonium-phenyl)-6-phenyl,1,3,5-hexatriene (TMA-DPH) fluorescence decay using distributional analysis

Journal

Chemistry and Physics of Lipids, 55(1)

ISSN

0009-3084

Authors

Zolese, Giovanna
Gratton, Enrico
Curatola, Giovanna

Publication Date

1990-07-01

DOI

10.1016/0009-3084(90)90146-i

Chemistry and Physics of Lipids, 55 (1990) 29—39
Elsevier Scientific Publishers Ireland Ltd.

Phosphatidic acid affects structural organization of phosphatidylcholine liposomes. A study of 1,6-diphenyl-1,3,5-hexatriene (DPH) and 1-(4-trimethylammonium-phenyl)-6-phenyl-1,3,5-hexatriene (TMA-DPH) fluorescence decay using distributional analysis

Giovanna Zolese[a], Enrico Gratton[b] and Giovanna Curatola[a]

[a]*Institute of Biochemistry, University of Ancona, Via Ranieri n. 65, 60131 Ancona (Italy) and* [b]*Laboratory for Fluorescence Dynamics, Department of Physics, University of Illinois, Urbana (U.S.A.)*

(Received August 8th, 1989; revision received December 4th, 1989; accepted February 20th, 1990)

The fluorescence decay of 1-(4-trimethylammonium-phenyl)-6-phenyl-1,3,5-hexatriene (TMA-DPH) was used to study microheterogeneity of 1,2-dimyristoyl-3-*sn*-phosphatidylcholine (DMPC) liposomes and to characterize the effect of phosphatidic acid on the correlation between fluorescence microheterogeneity and membrane permeability. The fluorescence decay, measured using multifrequency phase fluorometry, has been analyzed either by using a model of discrete exponential components or a model of continuous distribution of lifetime values. Both analyses have shown that TMA-DPH decay is characterized by two components: a long one of about 9 ns and a short one of about 5 ns. In the gel phase, at variance with previous DPH studies, the short component was associated with a large fractional intensity. The distributional analysis showed changes of lifetime values and width in correspondence to the calorimetric transitions. The presence of egg phosphatidic acid increased both long lifetime values and distributional width. The use of TMA-DPH as a probe to evaluate membrane heterogeneity using the distributional width is discussed. The effect of phosphatidic acid on the membrane surface and in the hydrophobic core has been related to its structural properties and to its role in water penetration.

Keywords: multilamellar vesicles; phosphatidic acid; DPH and TMA-DPH; frequency-domain fluorometry; fluorescence lifetime; continuous distribution analysis.

Introduction

The model of Singer and Nicolson [1] offered a general description of membrane organization but structural and functional aspects are unclear and still being debated. The complex membrane compositional pattern poses question as to the roles exerted by the different phospholipid species [2]; moreover, the stability of the bilayer configuration could depend on interacting forces related to the molecular shape of individual phospholipids [3]. Steric factors could be of functional relevance since they can favour bilayer/non-bilayer transitions and establish defects within the membrane bilayer where water and solute molecules could be located and, in general, cause membrane modifications leading to changes in mechanical properties [4]. A membrane model has been proposed in which structural heterogeneity could be an important membrane feature determining both specific physico-chemical properties in local microenvironments and being involved in functional events [5].

The physico-chemical changes introduced in the membrane bilayer by the presence of phosphatidic acid (PA) are interesting in several respects. PA, normally a minor component of cellular plasmamembranes [6], is rapidly accumulated following the activation of the phospha-

Correspondence to: Prof. Giovanna Curatola.

0009-3084/90/$03.50

tidylinositol cycle by a variety of functional stimuli [7,8], some of which involve fusional processes. PA has a characteristic configuration in the bilayer phase since its phosphatidic group packs with small cross section relative to the hydrocarbon chains; in pure PA liposomes and in mixtures, specific structural organization of PA occurs, in the range of physiological pH [9], probably through the formation of hydrogen bonds which link PA phosphate groups [10,11]. This behaviour modifies water organization at the membrane surface [9] and thermotropic properties of the membrane [12]. Moreover, in the presence of Ca^{2+} and other divalent cations, PA can assume non-bilayer configurations [2,13] relevant to aggregation and fusion phenomena. Although it has been proposed [14,15] that interaction of water molecules with phospholipid headgroups, dehydration processes and structural modifications at the membrane hydrophobic core are directly involved in the reorganization of membrane architecture during bilayer to non-bilayer transitions and fusion, knowledge of the molecular details, related to membrane structure and physico-chemical properties, is indirect and fragmentary.

The changes induced in membrane structural microheterogeneity, that is the formation of specific microenvironments, induced by the presence of negatively charged PA-containing unsaturated fatty acids, might be useful in investigating membrane properties at the surface and at the hydrophobic core, in relation to the aforementioned phenomena. We have approached this problem by studying the excited-state decay of a fluorescent probe 1,6-diphenyl-1,3,5-hexatriene (DPH) and its cationic derivative 1-(4-trimethylammonium-phenyl)-6-phenyl-1,3,5-hexatriene TMA-DPH) using frequency-domain fluorometry.

In previous works we have demonstrated, in liposomes [16] and in biological membranes [17,18], that the decay behaviour can be described by a continuous distribution of lifetime values whose width is related to the heterogeneity of the chemical and physico-chemical microenvironment of the probe. Therefore, such a distributional analysis represents a phenomenological approach to the study of membrane microheterogeneity. Since photophysical properties of TMA-DPH are similar to those of DPH we can assume that also TMA-DPH distribution analysis can reflect the heterogeneity of the probe surroundings. DPH lifetime is independent of environmental microviscosity but is strongly influenced by the dielectric constant [19] of the solvent. The relationship between average decay time and dielectric constant is a particularly useful property in our study since we have used a model membrane system in which the water penetration can be directly modified by PA. DPH localizes in the membrane hydrophobic core [20] while TMA-DPH is a charged probe located at the interfacial and headgroup surface [21]. Their parallel use on the same system allows the comparison of membrane structure at different depths in the bilayer.

Materials and methods

Egg phosphatidylcholine (EPC) and dimyristoylphosphatidylcholine (DMPC) were from Avanti Polar Lipids Inc. (Birmingham, AL) and egg phosphatidic acid (EPA) from Lipid Products (Redhill, Surrey, U.K.). The lipids were used without further purification. The background fluorescence was negligible in our experimental conditions. DPH and TMA-DPH were from Molecular Probes Inc. (Eugene, OR).

Preparation of multilamellar vesicles

Lipids suspended in chloroform or chloroform/methanol were mixed at the desired molar ratio. DPH in tetrahydrofuran solution or TMA-DPH in ethanol were added to obtain final probe: lipid molar ratio of 1/800 and the solution dried under nitrogen flux. Labelled multilamellar liposomes (MLV) were then formed by resuspending lipids, at a temperature well above the main phase transition (T_m), in 0.1 M NaCl, Tris/HCl 20 mM pH 7.4 to a final concentration of 0.4 mM in lipid.

Calorimetric measurements

Calorimetric data were obtained using a Perkin Elmer Calorimeter, model DSC-C2 with data

processor. Aluminium containers of 20 μl capacity were used. Lipid concentration was 142 mg/ml. The scan rate was 2.5°C/min on both heating and cooling cycles.

Fluorescence measurements

Steady-state fluorescence measurements were performed on a Perkin Elmer MPF66 fluorometer. Excitation and emission wavelengths were, respectively, 360 nm and 430 nm at bandwidths 5 nm. The scattering contribution to the measured signal was subtracted by using equivalent liposome suspensions without fluorescent probe. The temperature was controlled by using an external bath circulator and the actual sample temperature was measured in a reference cuvette using a digital thermometer.

Lifetime measurements were performed on a multifrequency phase fluorometer (ISS GREG200) interfaced with a M24 Olivetti computer for data collection and analysis. The excitation wavelength was 325 nm (UV line of an HeCd Liconix Model 4240 NB laser). A large range of modulation frequencies was used, between 2 and 130 MHz. POPOP in absolute ethanol (1.35 ns lifetime) was used as a reference [22]. Emission was collected through a Corion LG 370 S filter; data were accumulated until the standard deviations of phase and modulation values at a given frequency were below 0.1 and 0.002, respectively. The data analysis was performed by a non-linear least-squares routine for the multiexponential fit, described by Lakowicz [23] and a routine based on the simplex method for lifetime distribution analysis [24]. Following the calculation of Fiorini et al. [17] the reduced χ^2 value was used to judge the goodness of the fit. Given our uncertainty in the evaluation of the standard deviations of the individual points, a value of less than 3 was considered acceptable, while a value of the order of 10 indicated a large deviation between experimental and calculated values [23]. As discussed by Fiorini et al. [17], when using different functions for the fit the important parameter is the change in χ^2 rather than its absolute value.

Each experiment was repeated at least three times using independent preparations.

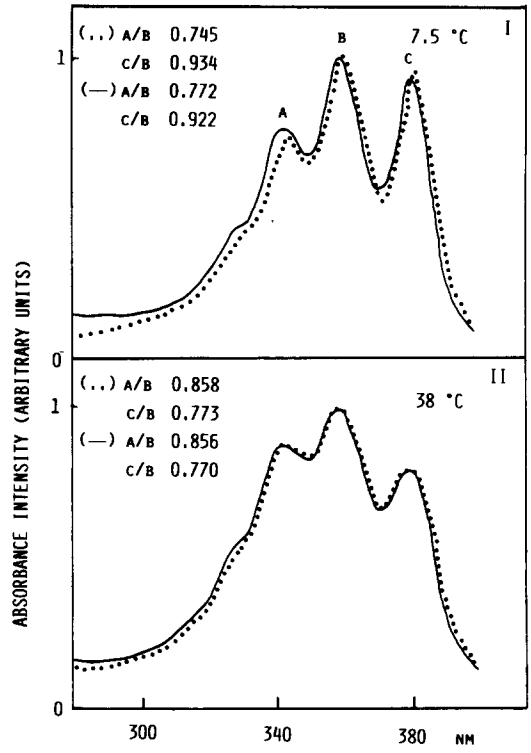

Fig. 1. Excitation spectra of TMA-DPH in DMPC (————) and DMPC/EPA (80/20 molar ratio) (·····). I, below main phase transition; II, above main phase transition. All the spectra are normalized to unity at the central peak (B).

Results

TMA-DPH fluorescence in DMPC and DMPC/EPA liposomes

Excitation spectra of TMA-DPH in DMPC and DMPC/EPA MLV, above and below the transition temperature from gel to liquid crystalline phases (T_m) are shown in Fig. 1. The spectrum obtained from the mixture in the gel phase shows different intensity ratios between peaks when compared with pure lipid. These differences are better evaluated by considering the ratio between peaks. Following the interpretation of Zannoni et al. [19] for DPH, below T_m the observed increase of C/B ratio and the parallel decrease of A/B ratio could be taken as an indication of polarity decrease. The changes in polarity are significant in the transition from gel

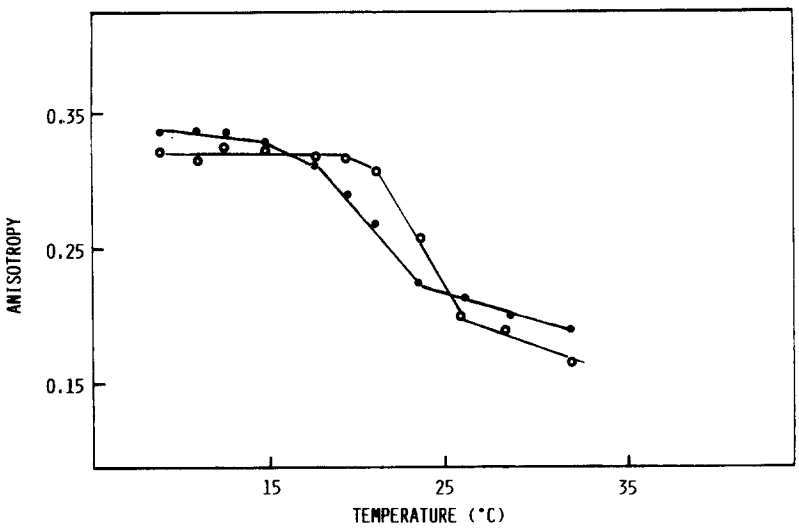

Fig. 2. Steady-state TMA-DPH fluorescence anisotropy in DMPC (O————O) and DMPC/EPA (80/20 molar ratio) (●————●) as a function of temperature.

to liquid crystalline state of both pure lipid and mixture. However, no difference was detectable between the two samples above T_m. A higher probe solubility due to differences in surface charge of MLV could be hypothesized but the absence of new peaks in the emission spectra (data not shown) led us to exclude the formation of excimer species.

The steady-state fluorescence anisotropy of TMA-DPH in DMPC and DMPC/EPA liposomes as a function of temperature is reported in Fig. 2. DMPC MLV exhibited an abrupt decrease of anisotropy between 22 °C and 23 °C, in agreement with calorimetric data (Fig. 4). The anisotropy values for DMPC/EPA show that in the mixture, the transition was shifted to lower temperature and the transition range was broader (15—22 °C) in agreement with data reported by Caffrey and Feigenson [25]. Moreover, above and below the DMPC/EPA transition, the anisotropy was higher than that observed in the corresponding phases for pure DMPC. Since the temperature range of the pure EPA phase transition was between 8 °C and 20 °C, our data indicated that the probe distribution could be considered homogeneous in the bilayer plane excluding the formation of EPA clusters in which TMA-DPH could be segregated.

The same MLV prepared for steady-state fluorescence studies were used for the measurements of TMA-DPH fluorescence decay. In DMPC MLV the exponential analysis gave an acceptable fit using two, but not one, components (Table IA). In the gel phase, while the short lifetime (about 5 ns) remained essentially constant, the long lifetime slightly increased from about 8.2 ns to about 9 ns with the temperature; moreover, temperature affected the fractional intensities associated with the two analyzed lifetimes. At temperatures higher than T_m, both long and short lifetimes decrease and the long component contributed almost all the intensity. Lorentzian distributional analysis (Table IB) showed similar results up to 13.3 °C. Above the calorimetric pretransition (Fig. 4) as well as in the liquid crystalline phase (L_α) the acceptable fits were obtained with a one component distributional analysis. The distribution width showed two changes at temperatures corresponding to the pre- and main transitions. Moreover the distributional approach gave an

TABLE I

Analysis of the fluorescence emission decay of TMA-DPH in DMPC[a]. (A) Two-component exponential analysis; (B) Lorentzian distribution of lifetime(s).

(A) Exponential analysis

T°C	F	τ_1	f_1	τ_2	χ^2
5.7	12	8.75 ± 0.21	0.57 ± 0.03	5.56 ± 0.14	1.85
8.4	13	8.11 ± 0.42	0.72 ± 0.11	4.45 ± 0.51	2.43
8.9	12	8.84 ± 0.38	0.63 ± 0.08	4.96 ± 0.31	0.89
13.0	11	8.32 ± 0.41	0.74 ± 0.10	4.37 ± 0.52	2.44
15.8	13	8.72 ± 0.33	0.60 ± 0.11	5.56 ± 0.30	2.86
16.7	12	8.93 ± 0.31	0.55 ± 0.07	5.59 ± 0.25	4.12
18.8	12	8.86 ± 0.31	0.57 ± 0.05	5.52 ± 0.22	4.80
19.7	12	8.68 ± 0.27	0.57 ± 0.07	5.56 ± 0.30	1.39
20.0	10	8.47 ± 0.34	0.52 ± 0.12	5.01 ± 0.28	4.49
25.4	14	6.13 ± 0.14	0.90 ± 0.03	2.09 ± 0.27	4.84
30.5	13	5.52 ± 0.11	0.92 ± 0.02	1.47 ± 0.20	6.48

(B) Lorentzian analysis

T°C	F	C_1	W_1	f_1	C_2	W_2	χ^2
5.7	12	8.45	0.170	0.623	5.50	0.05	1.825
8.4	13	8.11	0.220	0.640	5.16	0.05	2.263
8.9	12	8.70	0.090	0.65	4.96	0.05	0.927
13.0	11	8.34	0.100	0.730	4.53	0.05	2.558
15.8	13	7.30	0.575	—	—	—	2.23
16.7	12	7.23	0.637	—	—	—	3.89
18.8	12	7.22	0.579	—	—	—	3.59
19.7	12	7.17	0.551	—	—	—	1.87
20.0	10	6.58	0.650	—	—	—	2.19
25.4	14	5.58	1.208	—	—	—	1.142
30.5	13	5.09	1.413	—	—	—	2.05

[a] τ_1, τ_2, Lifetime in nanoseconds; f_1, fractional intensity; C_1, C_2, center of the distribution in nanoseconds; W_1, W_2, full width at half maximum of the distribution in nanoseconds; χ^2, reduced chi-square; F, number of frequencies.

improvement of the fit in the majority of cases, and the χ^2 values obtained were less variable.

In DMPC/EPA MLV, the exponential analysis (Table II) showed an increase in the absolute value and fractional intensity of the long lifetime component with respect to pure lipid MLV, and again, a short lifetime component needed to be included to obtain an acceptable fit. Distributional analysis gave, as in DMPC, lower value of χ^2 but a two-component distribution was necessary to describe the system adequately over the whole of the temperature range. Both long and short lifetimes and widths are sensitive to temperature. The average lifetime decreased as temperature increased, and the distribution width was larger above T_m, where the long component again contributed most of the intensity.

From a comparison of the TMA-DPH decay values obtained using distributional analysis in DMPC and DMPC/EPA MLV (Fig. 3 I,II) it was possible to evaluate the effect of EPA. Both the longer mean lifetime and its distributional width exhibited two abrupt changes corresponding to the pre-transition and transition tempera-

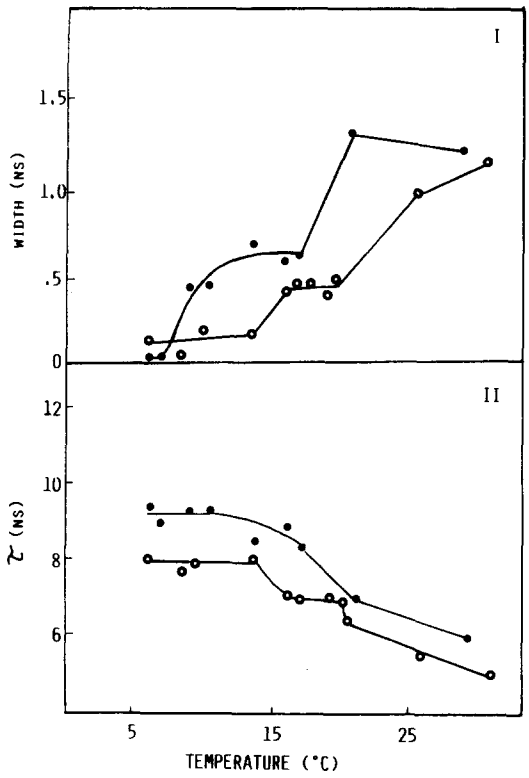

Fig. 3. Distributional analysis of TMA-DPH decay in DMPC (O———O) and DMPC/EPA (80/20 molar ratio) (●———●) MLV. I, long component distributional width; II, long component lifetime. Data presented are mean of three different experiments.

ture of DMPC. The presence of EPA increased the lifetime value of the long component and T_m was shifted to lower temperature (23 °C for DMPC; 19 °C for DMPC/EPA); a corresponding change was shown by the distributional width which was increased in DMPC/EPA with respect to pure DMPC, except at the extreme temperatures tested where the values were practically identical.

Changes of the thermotropic behaviour of DMPC induced by EPA as observed with the distributional analysis were also obtained by DSC: Fig. 4, II shows an enlarged and shifted main transition peak compared with pure DMPC (Fig. 4, I), but a clear separation between pre- and main transition is not possible. In a similar system, Caffrey and Feigenson [25] demonstrated by X-ray diffraction that the phase separation was minimal, suggesting a high degree of miscibility between the two lipids.

DPH fluorescence in DMPC and DMPC/EPA liposomes

As previously shown by Parasassi et al. [26], exponential analysis of DPH decay in DMPC can be adequately described by the sum of a long and a short component. In our experimental conditions (Table III), the lifetime values were respectively 9.58 ns and 3.90 ns in the gel phase and 8.16 ns and 2.61 ns in the liquid crystalline phase. The presence of EPA lengthened the long lifetime, and decreased its fractional intensity. The lifetime value of the short component was modified only in the gel phase. Distributional analysis also showed an increase in the long lifetime in presence of EPA, and

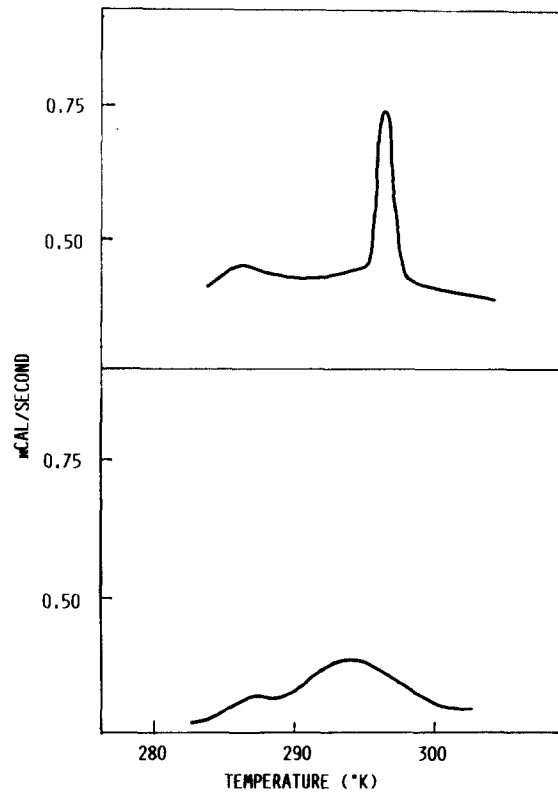

Fig. 4. DSC heating scans of DMPC (I) and DMPC/EPA (80/20 molar ratio) (II).

TABLE II

Analysis of the fluorescence emission decay of TMA-DPH in DMPC/EPA MLV (80/20 molar ratio)[a]. (A) Two-component exponential analysis; (B) Lorentzian distribution of lifetime.

(A) Exponential analysis

T°C	F	τ_1	f_1	τ_2	χ^2
5.4	12	9.86 ± 0.32	0.72 ± 0.06	5.5 ± 0.41	1.57
5.9	12	9.64 ± 0.31	0.82 ± 0.07	5.5 ± 0.40	4.34
6.8	12	9.57 ± 1.00	0.76 ± 0.26	5.8 ± 1.46	0.05
7.3	12	10.27 ± 0.34	0.74 ± 0.07	5.5 ± 0.40	2.79
8.9	12	10.29 ± 0.35	0.74 ± 0.07	5.6 ± 0.42	1.03
10.3	13	10.33 ± 0.30	0.68 ± 0.06	5.6 ± 0.29	0.65
15.8	11	10.34 ± 0.32	0.66 ± 0.06	5.5 ± 0.47	2.122
16.9	12	9.32 ± 0.32	0.79 ± 0.06	4.35 ± 0.41	2.456
20.8	13	7.89 ± 0.16	0.87 ± 0.02	2.36 ± 0.19	4.41
28.8	15	6.80 ± 0.16	0.82 ± 0.03	2.31 ± 0.17	4.93

(B) Lorentzian analysis

T°C	F	C_1	W_1	f_1	C_2	W_2	χ^2
5.4	12	9.76	0.05	0.73	5.5	0.05	1.87
5.9	12	9.51	0.05	0.82	5.3	0.08	5.97
6.8	12	9.51	0.05	0.77	5.58	0.05	6.02
7.3	12	9.77	0.785	0.77	6.06	0.05	2.32
8.9	12	9.66	0.563	0.82	5.60	0.05	0.77
10.3	13	9.63	0.637	0.78	5.64	0.05	0.46
15.8	11	9.46	0.787	0.77	5.5	0.05	1.81
16.9	12	8.55	0.902	0.90	4.35	0.05	2.043
20.8	13	7.03	1.799	0.97	1.37	2.281	0.849
28.8	15	5.98	1.531	0.95	2.31	1.491	1.873

[a]See footnote to Table I.

below T_m the best fit was obtained with one component only for pure lipid MLV, while in the mixture, the decay was always described by two components. In agreement with our previous data for DPH in DMPC [17], the distribution width decreased from gel to liquid crystalline phase; an opposite behaviour was observed for distribution width in the mixture. It was very narrow in the gel phase and enlarged in the liquid-crystalline state, suggesting that EPA presence induces changes in the probe microenvironments.

TMA-DPH and DPH fluorescence in EPC and EPC/EPA liposomes

To evaluate better the influence of unsaturation and chain lengths of EPA and to clarify the effect of charged headgroup on such a bilayer structure, we performed fluorescence decay studies in EPC/EPA MLV which are rich in unsaturated fatty acyl chains of variable length, at a temperature well above T_m for the whole compositional range.

Acceptable fits (Table IV, A,B) were obtained with exponential analysis using two, but not

TABLE III

Fluorescence emission decay of DPH in DMPC and DMPC/EPA (80/20 molar ratio) MLV. (A) Exponential analysis; (B) Lorentzian distribution of lifetime.

(A)

	τ_1	f_1	τ_2	χ^2
7.7°C				
DMPC	9.96 ± 0.50	0.87 ± 0.13	5.59 ± 1.37	1.953
DMPC/EPA	12.41 ± 0.47	0.84 ± 0.04	4.53 ± 0.54	0.680
27°C				
DMPC	8.13 ± 0.08	0.95 ± 0.01	2.45 ± 0.35	1.13
DMPC/EPA	9.80 ± 0.14	0.92 ± 0.01	2.77 ± 0.24	2.52

(B)

	C_1	W_1	f_1	C_2	W_2	χ^2
7.7°C						
DMPC	9.222	0.604	—	—	—	1.799
DMPC/EPA	12.12	0.100	0.85	4.87	0.05	0.768
27°C						
DMPC	8.09	0.200	0.95	2.68	0.98	1.22
DMPC/EPA	9.55	0.623	0.94	2.76	0.42	2.33

TABLE IV

Biexponential analysis of DPH (A) and TMA-DPH (B) fluorescence decay in liposomes with increasing content of PA. T = 20°C.

	τ_1	f_1	τ_2	χ^2
(A) DPH				
100/0	7.99 ± 0.10	0.95 ± 0.01	2.25 ± 0.27	1.285
95/5	8.59 ± 0.09	0.92 ± 0.01	2.14 ± 0.15	0.948
90/10	8.72 ± 0.09	0.93 ± 0.09	2.37 ± 0.17	1.018
85/15	8.61 ± 0.09	0.95 ± 0.08	1.99 ± 0.21	1.275
80/20	8.77 ± 0.09	0.95 ± 0.07	1.87 ± 0.17	0.948
(B) TMA-DPH				
100/0	3.94 ± 0.08	0.85 ± 0.03	1.42 ± 0.12	1.89
95.5	4.03 ± 0.03	0.92 ± 0.05	0.70 ± 0.05	0.93
85/15	4.12 ± 0.08	0.88 ± 0.01	0.85 ± 0.10	1.37
80/20	4.20 ± 0.04	0.93 ± 0.07	0.71 ± 0.07	2.22

one, components, most of the fractional intensity being associated with the long component, both for DPH and TMA-DPH. In both cases the presence of EPA in the highly unsaturated MLV induced only a slight increase in the long lifetime.

Discussion

TMA-DPH is localized at the interface of the bilayer [21,27] and probes a region of high water penetration [28]. The fluorescence lifetime of TMA-DPH is longer when the probe is embedded in a lipid bilayer than in solution, suggesting a quenching effect by water molecules [27]. Its photophysical properties are generally similar to those of DPH [21], and we assume that its lifetime is sensitive to the dielectric constant in the same way as that of DPH.

To evaluate the role of phospholipid polar headgroups and fatty acyl chains on membrane heterogeneity we have used liposomes prepared from saturated and unsaturated phosphatidylcholine with EPA.

PA headgroups are linked by intermolecular hydrogen bonding, occurring also in excess water, at physiological pH, despite the presence of a negative charge. The small cross-section of the phosphate group cannot tightly cover the layer surface [9], so that water molecules have to be accommodated as spacer molecules into the polar headgroup region [11]. It was suggested that, in a biological membrane, PA forms hydrogen bonded dimers [30] or strands [11]. On the other hand, the hydrogen bonding PA packs more closely than PC in a monolayer [9]. This is due to the strong intermolecular hydrogen bonds [9], formed in PA between phosphate groups. These interactions between —PO groups, that are the most likely candidate for water binding in phospholipids (PL) [11], could prevent high PA hydration, as suggested for other hydrogen bonded molecules [31]. In contrast, PC molecules are bonded together through water molecules [31]. This particular arrangement would explain the lower polarity detected as changes of TMA-DPH spectra (Fig. 1) in the presence of EPA, evident in the gel phase. In our experimental conditions a complete miscibility of DMPC and EPA is suggested by anisotropy data, in agreement with Caffrey and Feigenson [25]. As for DPH, TMA-DPH fluorescence decay requires at least two exponentials for adequate description. In pure lipid the long component is sensitive to the transition from gel to liquid crystalline state and the decrease of its absolute value can be interpreted, as for DPH [16], as due to an increase of dielectric constant caused by water redistribution in the bilayer following the transition [28]. At variance with DPH, below T_m, a large part of the fractional intensity is associated with the short lifetime component. The origin of the short component has been extensively discussed and assigned variously to a fraction of photolytic products [26], to probe molecules located in a very polar environment at the membrane surface [33], or to defects between membrane domains [33]. Up to 13 °C the center values of the two distributed components are similar to the values of the long and short components of the exponential analysis. At higher temperatures a single distribution is enough to obtain a good fit. Using the distributional analysis, the center lifetime value shows two decreases at definite temperatures related to pre-transition and main transition. The width of the lifetime distribution increases as the temperature is increased. For DPH [16], the width of the distribution can be taken as an indication of the degree of membrane heterogeneity related to structural defects which induce microenvironments of different dielectric constant. The narrowing of the distribution width for DPH above T_m has been ascribed to diffusion during the excited-state lifetime. For TMA-DPH, below the pre-transition, the presence of two components, both with large fractional intensity, may indicate two different sets of microenvironments for TMA-DPH.

The broad distribution of the single lifetime observed at temperatures above the transitions might be explained by the relative fixed position of this probe which cannot experience rapid movements perpendicular to the membrane plane during the fluorescence lifetime, such as proposed for DPH.

Recently, a more complex spectroscopic model for DPH decay has been proposed [36], involving two different excited states of DPH with different fluorescence lifetimes. The surrounding medium affects the rate of interconversion between these states. In this model, the different decay times can arise from a single environment in which the barrier for interconversion between the two states is relatively large. In the presence of EPA, both the exponential and distributional analyses show an increase in the long lifetime value, which is sensitive only to changes occurring at the main transition.

A short component is necessary to obtain a good fit with the distributional analysis and its central value and the width are modified, following the transition. This behaviour suggests a different pattern of heterogeneity introduced by the unsaturated PA, as previously discussed in agreement with previous interpretation the TMA-DPH distribution width is related to its limited mobility perpendicular to the membrane. The different spectroscopic properties observed in the two phospholipid systems used imply a different penetration of water molecules. The heterogeneity, due to the presence of EPA, would have to be homogeneously distributed in the plane of the bilayer since phase separation has not been demonstrated. Our interpretation on the decrease of water penetration inside the bilayer is confirmed by the increase in lifetimes of both long and short components observed for DPH above and below T_m in the presence of EPA, although generally the unsaturation of hydrocarbon chains, which weakens headgroup interactions, increases chain mobility and water penetration [39—41]. However, Davenport et al. [20] have suggested a limited vertical mobility of DPH which locates in a restricted area in the central part of the bilayer in the case of unsaturated phospholipid. Both these interpretations might explain the narrow lifetime distribution width below the transition, the broadening in the liquid crystalline state for EPA suggests an increase in the number of defects, i.e. heterogeneity, due to unsaturation compared with those related to the mobility of saturated chains. The lifetime increase observed in highly unsaturated liposomes in the liquid crystalline state, as in EPC containing EPA at increasing concentrations, supports the interpretation that EPA modifies the membrane polarity profile. The decay behaviour of TMA-DPH and DPH, studied by lifetime distributional analysis, allows a detailed characterization of polarity changes induced in the membrane by the presence of EPA both at the membrane surface and in the hydrophobic core. Altogether, our observations support in part the "rectangular" model of water distribution (for an extensive review see Deamer and Bramhall [28]). However, occasional molecules of water are found beyond the carbonyl oxygen, and their number increases with temperature and/or with the number of structural defects.

Acknowledgements

This work was supported by grants CNR No. 89.0291.04, 60% (G.C.) and NIH RR03155 (E.G.).

References

1 S.J. Singer and G.L. Nicolson (1972) Science 175, 720—731.
2 P.R. Cullis, B. De Kruijff, M.J. Hope, A.J. Verkleij, R. Nayar, S.B. Farren, C. Tilcock, T.D. Madden and M.B. Bally (1983) in: R.C. Aloia (Ed.), Membrane Fluidity in Biology, Academic Press, New York, pp. 40—81.
3 J.N. Israelachvili, S. Marcelja and R.G. Horn (1980) Quart. Rev. Biophys. 13, 121—125.
4 G. Curatola and G. Lenaz (1987) in: N. Akkas (Ed.), Biomechanics of Cell Division, Plenum Press, New York, pp. 33—77.
5 G. Curatola and E. Bertoli (1987) In: E. Bertoli, D. Chapman, A. Cambria and U. Scapagnini (Eds.), Biomembrane and Receptor Mechanisms, Springer Verlag/Liviana Press, Padova, pp. 143—161.
6 G.B. Ansell, J.N. Hawthorn and R.M. Dawson (1973) in: G.B. Ansell (Ed.), Form and Function of Phospholipids, Elsevier, Amsterdam, pp. 28—38.
7 M.J. Broekman, J.W. Ward and A.J. Markus (1980) J. Clin. Invest. 66, 275—280.
8 M.J. Berridge (1987) Annu. Rev. Biochem. 56, 159—193.
9 J.M. Boggs (1987) Biochim. Biophys. Acta 906, 353—404.
10 K. Jacobson and D. Papahadjopoulos (1975) Biochemistry 14, 152—161.

11 K. Harlos, H. Eibl, I. Pascher and S. Sundell (1984) Chem. Phys. Lipids 34, 115—126.
12 H. Eibl and A. Blume (1979) Biochim. Biophys. Acta 553, 476—488.
13 S.B. Farren, M.J. Hope and P.R. Cullis (1983) Biochem. Biophys. Res. Commun. 111, 675—682.
14 R. Sundler (1984) in: M. Kates and L.A. Manson (Eds.), Biomembranes, Plenum Press, New York, pp. 563—583.
15 E. Sackmann (1984) in: M. Shinitzky (Ed.), Biological Membranes, Academic Press, New York, pp. 106—143.
16 R.M. Fiorini, M. Valentino, E. Gratton, E. Bertoli and G. Curatola (1987) Biochem. Biophys. Res. Commun. 147, 460—466.
17 R.M. Fiorini, M. Valentino, S. Wang, M. Glaser and E. Gratton (1987) Biochemistry 26, 3864—3870.
18 R.M. Fiorini, M. Valentino, M. Glaser, E. Gratton and G. Curatola (1988) Biochim. Biophys. Acta 939, 485—492.
19 C. Zannoni, A. Arcioni and P. Cavatorta (1983) Chem. Phys. Lipids 32, 179—184.
20 L. Davenport, R.E. Dale, R.H. Bisby and R.B. Cundall (1985) Biochemistry 24, 4097—4108.
21 F.G. Prendergast, R.P. Haughland and P.J. Callahan (1981) Biochemistry 20, 7333—7338.
22 J.R. Lakowicz, H. Cherek and A.J. Balter (1981) Biochem. Biophys. Methods 5, 131—141.
23 J.R. Lakowicz, G. Laczko, H. Cherek, E. Gratton and M. Limkeman (1984) Biophys. J. 46, 463—477.
24 J.M. Alcalà, E. Gratton and F.G. Prendergast (1987) Biophys. J. 51, 587—596.
25 M. Caffrey and G.W. Feigenson (1984) Biochemistry 23, 323—331.
26 T. Parasassi, F. Conti, M. Glaser and E. Gratton (1984) J. Biol. Chem. 259 14011—14017.
27 M. Straume and B.J. Litman (1987) Biochemistry 26, 5113—5120.
28 D.W. Deamer and J. Bramhall (1986) Chem. Phys. Lipids 40, 167—188.
29 A.G. Lee (1977) Biochim. Biophys. Acta 472, 285—344.
30 S. Massari and D. Pascolini (1977) Biochemistry 16, 1189—1195.
31 J.H. Crowe and L.M. Crowe (1984) in: M. Shinitzky (Ed.), Biological Membranes, Academic Press, New York, pp. 57—103.
32 P.T.T. Wong and H.H. Mantsch (1988) Chem. Phys. Lipids 46, 213—224.
33 M.J. Karnovsky, A.M. Kleinfeld, R.L. Hoover and R.D. Klausner (1981) J. Cell. Biol. 94, 1—6.
34 E. Sackmann, D. Ruppel and C. Gebhardt (1980) in: W. Helfrich and G. Heppke (Eds.), Chemical Physics, Springer Verlag, New York, pp. 309—326.
35 M.J. Janiak, D.M. Small and G.G. Shipley (1976) Biochemistry 15, 4575—4580.
36 T. Parasassi and E. Grayton (1989) in: Membrane Technology, Serono Symposia, Raven Press, N.Y., 64, 109—117.
37 H. Hauser, I. Pascher, R.H. Pearson and S. Sundell (1981) Biochim. Biophys. Acta 650, 21—30.
38 S. Simon, T.J. McIntosh and R. La Torre (1982) Science 216, 65—67.
39 R.A. Demel, K.R. Bruckdorfer and L.L.M. Van Deenen (1972) Biochim. Biophys. Acta 255, 321—330.
40 G.L. Jendrasiak and J.H. Hasty (1974) Biochim. Biophys. Acta 348, 45—54.
41 G.L. Jendrasiak and J.H. Hasty (1974) Biochim. Biophys. Acta 337, 79—91.